Hybrid Power Filter to Enhance Power Quality in a Medium-Voltage Distribution Network

Victor Fabián Corasaniti, *Member, IEEE*, Maria Beatriz Barbieri, *Senior Member, IEEE*, Patricia Liliana Arnera, *Senior Member, IEEE*, and María Inés Valla, *Senior Member, IEEE*

***Abstract*—This paper deals with the problem of reactive power and harmonics in a standard medium-voltage (MV) distribution network. It proposes a simple and inexpensive solution to enhance power quality when a particular connection to the high-voltage transmission network is required. It presents the design of a hybrid active filter topology connected to the MV level of a power distribution system. Its main task is to regulate a 132-kV voltage level. Reconfiguration of the power delivery network imposes new constraints in a distribution substation so that the reactive compensation should be increased. The topology of a shunt hybrid active filter is analyzed. It is built with the series connection of a passive filter and a low-rated active filter. The proposed filter is directly connected to a 13.8-kV level with no need of a step-down transformer. The possibility of different levels of reactive power compensation is implemented. The proposal shows very good performance for different load demands.**

***Index Terms*—Active filters, harmonic distortion, power distribution, power quality, reactive power.**

I. Introduction

THE NONLINEAR loads and equipment in the consumer side and the renewable energy sources in the generation side give birth to new problems in electrical systems. Then, power electronics appears as an essential interface to improve power quality [1], [2]. Voltage distortion, due to current harmonics, has become a major problem for the utilities at distribution levels. Utilities frequently encounter harmonic-related problems such as harmonic interactions between utility and loads, reduced safe-operating margins, reactive power, resonance problems, higher transformers and line losses, and derating of distribution equipment [1], [3].

The use of traditional compensation with capacitor banks and passive filters produces harmonic propagation, i.e., harmonic voltage amplification due to the resonance between line inductances and shunt capacitors. Therefore, different active solutions have been continuously analyzed in recent years [4]–[6]. A lot of research on different topologies has been done to improve power quality [5]. The correct placement of the active filters in a distribution system has been investigated [7]. A lot of care is taken on different control strategies to obtain the desired objectives [8]–[13].

The feasibility of using an active solution to solve a particular problem of an actual power distribution grid is considered in this paper. Reconfiguration of the network imposes new constraints on different distribution substations (DSs). Harmonic studies were performed considering the future configuration of the network. Voltage distortions in different points of the network, together with the working conditions of the capacitor banks, were verified by means of harmonic flow [14]. A preliminary proposal suggested increasing the existing passive compensation with capacitor banks from 3 to 6 Mvar, but this solution introduced resonances near the fifth and seventh harmonics, resulting in unacceptable distortion levels. A second proposal (analyzed in [15]) considered a pure shunt active power filter. This, being an excellent solution when the load can be modeled as harmonic current sources, is not so effective when the load presents certain impedances as usual. Therefore, a hybrid solution is proposed here to solve the particular problem of enhancing the 132-kV level in a radial connection of the medium-voltage (MV) network.

Among all the compensation alternatives, the hybrid topologies appear very attractive in the distribution networks where some passive compensation is already installed. In particular, the hybrid shunt active filter formed with the connection of a low-rate active filter in series with one or several passive filters is gaining attention [4], [16]–[19]. Such a combination between active and passive filters allows significantly reducing the rating of the active filter. Its main tasks are to improve the filtering performance and to avoid the resonance problems introduced by passive filters. Moreover, no extra components are required to filter the ripple caused by the power inverter. It constitutes a simple and cheap solution for harmonics in a power distribution network.

This paper is organized as follows. The network configuration and the harmonic problems are described in Section II. The shunt hybrid active power filter (SHAPF) is analyzed in Section III. Section IV presents the design of the hybrid filter. Its performance is evaluated in Section V. Finally, conclusions are drawn in Section VI.

II. Network Description

The 132-kV network, where the DSs under study are connected, is a meshed network connected to the 500-kV high-voltage transmission system through two points. In the

Manuscript received July 4, 2007; revised January 16, 2009. First published February 6, 2009; current version published July 24, 2009. This work was supported in part by the IITREE—Facultad de Ingeniería—Universidad Nacional de La Plata (UNLP), by the FONCyT-ANPCyT, and by the Consejo Nacional de Investigaciones Científicas y Técnicas (CONICET).

V. F. Corasaniti, M. B. Barbieri, and P. L. Arnera are with the IITREE-LAT, Facultad de Ingeniería, Universidad Nacional de La Plata (FI-UNLP), 1900 La Plata, Argentina (e-mail: iitree@iitree-unlp.org.ar).

M. I. Valla is with the Consejo Nacional de Investigaciones Científicas y Técnicas, 1033 Buenos Aires, Argentina, and also with the Laboratorio de Electrónica Industrial, Control e Instrumentación, Departamento de Electrotecnia, Facultad de Ingeniería, Universidad Nacional de La Plata, 1900 La Plata, Argentina (e-mail: m.i.valla@ieee.org).

Digital Object Identifier 10.1109/TIE.2009.2014369

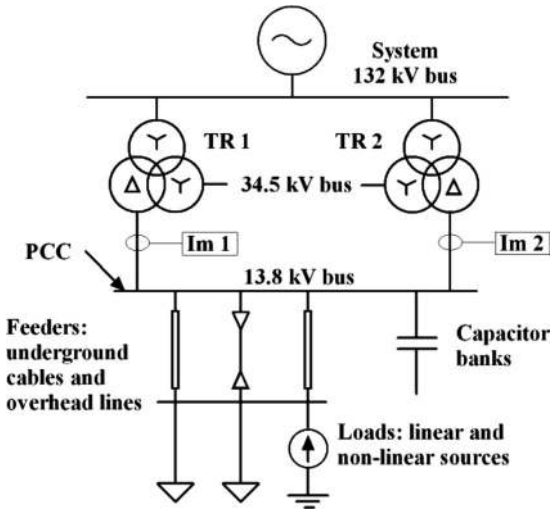

Fig. 1. One-line diagram of network model.

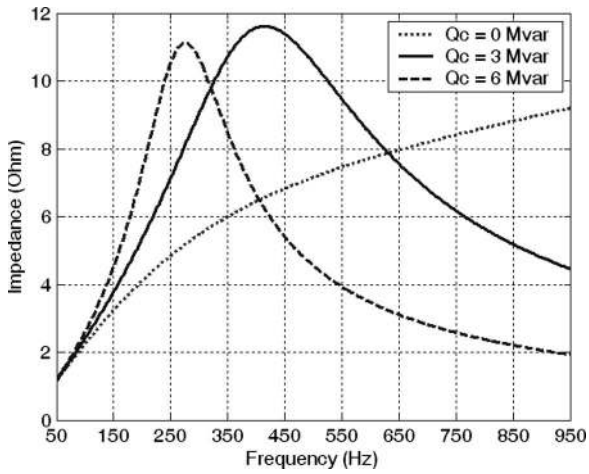

Fig. 2. Frequency response in 13.8-kV bus.

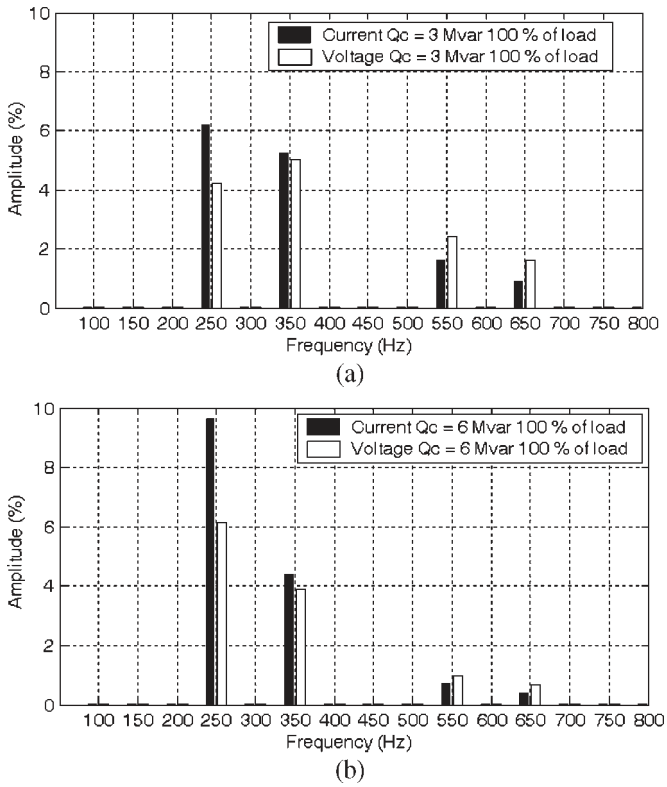

Fig. 3. Magnitude of current and voltage harmonics at the 13.8-kV bus. (a) $Q_C = 3$ Mvar. (b) $Q_C = 6$ Mvar.

future, it will be necessary to work in a radial network connected to the 500-kV system at only one point. The requirement to enhance the voltage profile at 132-kV level, far away from the 500-kV connection, demands new compensation in the different substations [14]. The loads of the different substations are mainly commercial and residential, so it is more difficult to identify the harmonic sources than in the case of industrial plants. Then, it is necessary to build a model based on the field measurements.

Fig. 1 shows the one-line diagram of the network model adopted for the DS under test. A digital three-phase model of the network is constructed using MATLAB/Simulink power system blockset. The system is represented as an ideal voltage source of 132 kV connected to two transformers of similar characteristics, 132/34.5/13.8 kV and 15/10/15 MVA. There are no loads at the 34.5-kV level. Both transformers are connected in parallel to 13.8 kV where the capacitor banks are placed. The short circuit power at 13.8 kV is approximately 150 MVA. Based on the power flow and harmonic studies performed on the network [14], the power demand considered in this model is 20.9 MVA with $\cos\varphi = 0.78$. The harmonic peak currents are $I_5 = 50.3$ A, $I_7 = 35.1$ A, $I_{11} = 15.1$ A, and $I_{13} = 11.4$ A, resulting in a total harmonic distortion of $THD_I = 5\%$. The goal of the proposed compensator, cos $\varphi = 0.92$ at 13.8 kV, is obtained with a reactive compensation of $Q_C = 6$ Mvar.

A. Harmonics

The interaction between the capacitance of the banks and the short circuit inductance of the network produces resonances at different frequencies depending on the compensation level. This was confirmed with a power flow of the system and the frequency response of the simplified model designed for the simulations as shown in Fig. 2.

It is evident that in both cases, the resonance frequencies enhance the most important current harmonics such as 5th (250 Hz), 7th (350 Hz), and 11th (550 Hz). Fig. 3(a) and (b) shows the current and voltage harmonics at the 13.8-kV bus, expressed as a percentage of the fundamental value. Both alternatives of capacitor banks, $Q_C = 3$ Mvar and $Q_C = 6$ Mvar, with 100% of load are considered.

TABLE I
POWERS AND POWER FACTOR RESULTS

Q_c (Mvar)	P (MW)	Q (Mvar)	V_{1phase} (kV rms)	THD_V (%)	I_{1line} (A rms)	THD_I (%)	Pf_{tot}	Q_{Ac} (Mvar)
0	16.3	13	7723	4.86	902.9	5.03	0.78	0
3	17	10.55	7864	7.2	848.1	8.32	0.85	2.95
6	17.65	8	8010	7.38	804.6	10.6	0.9	6

The results of these compensations at the 13.8-kV bus are summarized in Table I. It shows P and Q as defined in [20], the current and voltage fundamental values, their total harmonic

TABLE II
RESULTS AND VERIFICATIONS

Harmonic voltages	Q_c 0 Mvar	Q_c 3 Mvar	Q_c 6 Mvar	IEEE limits
V_5 (%)	2.95	4.24	**6.15**	3
V_7 (%)	2.85	**5.03**	3.91	3
V_{11} (%)	1.95	2.42	0.99	3
V_{13} (%)	1.75	1.61	0.65	3
THD_V (%)	4.86	7.2	7.38	5

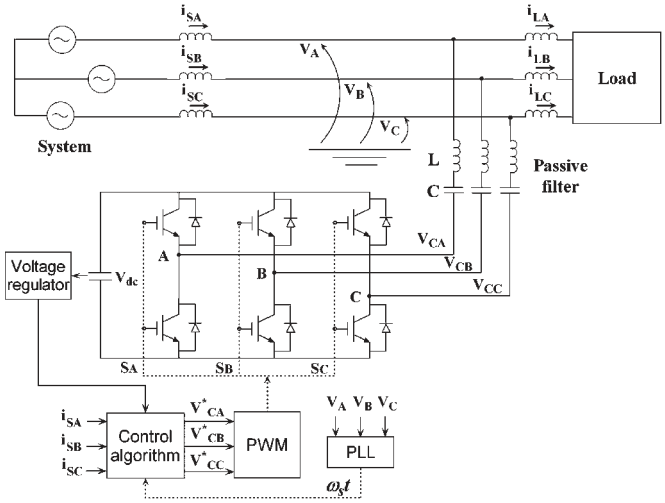

Fig. 4. Structure of the proposed SHAPF.

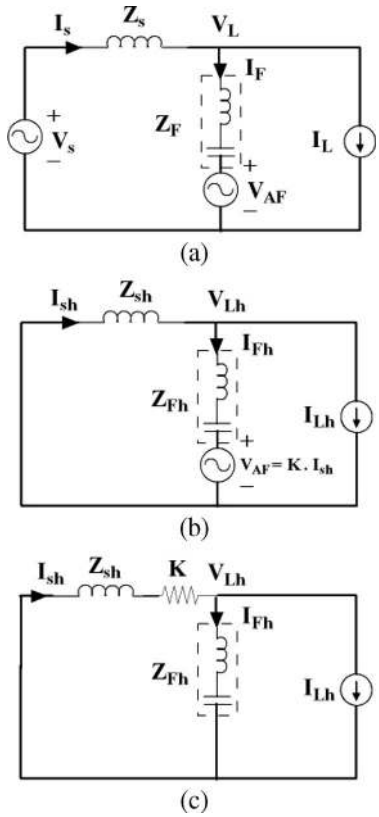

Fig. 5. Single-phase equivalent circuits of the system with hybrid active power filter connected. (a) Total equivalent circuit. (b) Equivalent circuit for harmonic components. (c) Resistive equivalence of the harmonic filter.

distortions, the power factor, and the reactive power provided by capacitor banks ($Q_{\rm AC}$).

Table II summarizes the voltage harmonics for $Q_C =$ 0 Mvar, $Q_C = 3$ Mvar, and $Q_C = 6$ Mvar compensation with full load, together with the limits fixed by IEEE [21].

In both cases, the individual voltage harmonics for the fifth and the seventh harmonics are above the allowable levels, so a different compensation should be considered.

III. HYBRID ACTIVE FILTER COMPENSATION

The structure of the proposed SHAPF is shown in Fig. 4. It consists of a three-phase pulsewidth-modulation (PWM) voltage source inverter (VSI) connected in series with one or more passive filters. They are directly connected to the grid without the need of a transformer. The passive filters consist of simple LC filters per phase tuned near certain harmonic frequencies. Basically, the active power filter acts as a controlled voltage source which forces the system line currents to become sinusoidal.

The hybrid active filter basically consists of a passive filter connected in series with a controlled voltage source as shown by the single-phase equivalent circuit in Fig. 5(a). The active filter is used only to compensate harmonics, while the reactive currents are damped by the passive filters. Therefore, it is considered as a voltage source proportional to the harmonic line currents ($V_{\rm AF} = K \cdot I_{\rm Sh}$), where K is the gain of the active filter. The load is assumed to be an ideal current source I_L, and Z_F is the impedance of the LC filter.

When no active filter is connected ($K = 0$), the ratio between the harmonic components of the ac line current ($I_{\rm Sh}$) and those of the nonlinear load ($I_{\rm Lh}$) is easily obtained from Fig. 5(b), considering the ac mains (V_s) as purely sinusoidal

$$\frac{I_{\rm Sh}}{I_{\rm Lh}} = \frac{Z_{\rm Fh}}{Z_{\rm Fh} + Z_{\rm Sh}}. \tag{1}$$

A good filtering is obtained only when $Z_{\rm Fh} \ll Z_{\rm Sh}$. However, this is not always the case for all the harmonics generated by the load. Moreover, harmonic resonances between Z_S and Z_F may occur at specific frequencies, thus causing the so-called harmonic amplifying phenomena.

When the active filter is connected, the ratio ($I_{\rm Sh}/I_{\rm Lh}$) becomes

$$\frac{I_{\rm Sh}}{I_{\rm Lh}} = \frac{Z_{\rm Fh}}{K + Z_{\rm Fh} + Z_{\rm Sh}}. \tag{2}$$

Equation (2) defines the filtering characteristic of the hybrid topology ($I_{\rm Sh}/I_{\rm Lh}$), which depends on the value of the passive filter equivalent impedance $Z_{\rm Fh}$, the system impedance $Z_{\rm Sh}$, and the active power filter gain K. It shows that the active filter behaves as a pure resistor of value $K(\Omega)$ connected in series with $Z_{\rm Sh}$ as shown in Fig. 5(c). If K is much bigger than $|Z_{\rm Fh}|$, all the harmonic currents injected by the load would flow into the passive filter. When K is also much bigger than $|Z_{\rm Sh}|$, K would dominate the filtering characteristics of the whole compensator. Moreover, K acts as a resistor which damps possible parallel resonances between Z_S and Z_F. A high value of K improves the compensation performance of the filter. It

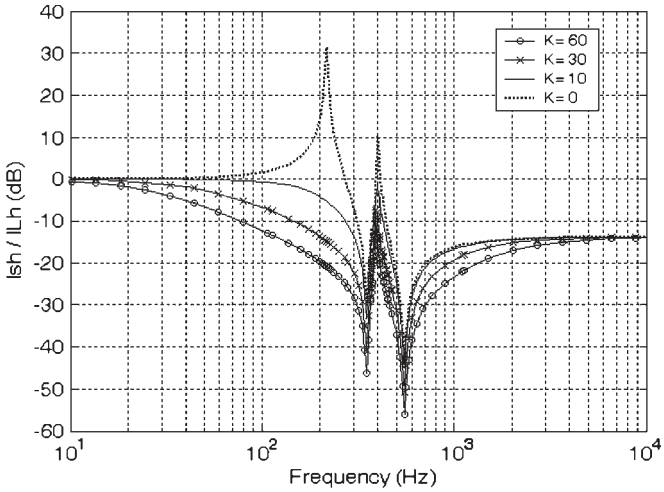

Fig. 6. Filtering characteristics of the hybrid filter.

helps the passive filter to absorb the load harmonic current I_{Lh}, so that only a small amount of it flows through the supply.

Fig. 6 shows the relationship between I_{Sh} and I_{Lh} for different values of K. The Z_S of the system under test is considered together with the Z_F of two passive filters tuned at 7th and 11th harmonics which compensate $Q_C = 3$ Mvar each. It should be remarked that K is null at fundamental frequency.

Fig. 6 shows the two resonance frequencies of the passive filters, i.e., 350 and 550 Hz. When no active filter is connected $(K = 0)$, harmonic amplification appears between 100 and 400 Hz. On the other hand, when the active filter is connected $(K > 0)$, no harmonic amplification occurs and the harmonic damping increases with greater values of K.

IV. Design of Hybrid Active Filter

The control system has two main tasks when generating the voltage references to the PWM VSI: 1) Eliminate the harmonics from the line currents, and 2) control the dc voltage of the VSI. Therefore, the analysis and design of the SHAPF may be divided into three main sections: the passive filter, the PWM VSI, and the control block.

A. Passive Filter

The passive filter has three main functions: reactive compensation, absorption of harmonic currents produced by the load, and coupling of the inverter to the grid. Since the load is variable, it is advisable to have different levels of reactive compensation. Equation (1) suggests that the passive filter should have the lowest possible impedance at the 5th, 7th, 11th, and 13th harmonic frequencies to achieve good filtering characteristics. However, implementing four passive filters would be bulky and expensive. Then, two passive filters tuned at 7th and 11th harmonics are also recommended to provide 3 Mvar each. The main reasons for this selection are as follows.

1) The LC filter tuned at the 7th and 11th harmonic frequencies is less bulky and expensive than the one tuned at the 5th and 7th harmonics.

TABLE III
Passive Filter Parameters

7^{th} Passive filter				11^{th} Passive filter			
Q_c (Mvar)	3	C_F (uF)	50	Q_c (Mvar)	3	C_F (uF)	50
f_r (Hz)	350	L_F (mH)	4.12	f_r (Hz)	550	L_F (mH)	1.67
Q	45	R_F (ohm)	0.2	Q	45	R_F (ohm)	0.315

2) The filter tuned at the 11th harmonic presents lower impedance at the 13th harmonic than another tuned at the 7th harmonics.

The level of reactive power defines the capacitance C_F of both filters. Therefore, once the reactive power compensation (Q_c), the tuned harmonic frequency (f_r), and a typical quality factor (Q) of each passive filter have been defined, the values of $C_F(\mu\mathrm{F})$, $L_F(\mathrm{mH})$, and $R_F(\Omega)$ are calculated [3]. Table III summarizes the parameters of the passive filters.

B. PWM VSI

The PWM VSI is a standard two-level three-phase VSI with IGBTs [2], [22]–[25] using a standard sinusoidal modulation with a carrier frequency of 10 kHz.

The inverter is connected to the 13.8 kV bus or point of common coupling (PCC) through the passive filters. Since the LC filter presents high impedance at the switching frequency, no extra components are required to filter the ripple produced by the inverter output voltage. In addition, the inductors of each passive filter function like coupling inductors to connect the converter to the network. Therefore, the passive filter tuned at the lowest frequency is connected first in order to better filter the harmonics generated by the PWM.

The dc side of the converter is built only with a capacitor of proper value. The capacitance is selected in order to keep the voltage ripple below 1%. The dc value is chosen so that the converter can supply the current time derivatives demanded by the harmonics to be compensated. Consequently, when higher harmonics are required for the SHAPF, the voltage level in the dc side, the voltage rating for the power IGBTs, and the switching frequency required to follow the reference currents are higher. The active filter can build up and regulate the dc voltage on the capacitor without any external power supply or special start-up circuit. The dc voltage level is controlled with a proportional controller. The inverter design values are $V_{\mathrm{dc}} = 1500$ V and $C = 5000$ μF.

C. Control-System Reference-Voltage Generator

The control system measures the three-phase currents at the secondary windings of the transformers (Im1 and Im2 in Fig. 1). Then, the supply currents (i_{SA}, i_{SB}, i_{SC}) are obtained by summing Im1 and Im2. With the three-phase supply currents (i_{SA}, i_{SB}, i_{SC}), the three-phase supply voltages (v_A, v_B, v_C), and the dc voltage of the inverter, the control builds the reference voltages for the PWM VSI.

First, the three-phase supply currents (i_{SA}, i_{SB}, and i_{SC}) are transformed into the instantaneous active (i_d) and reactive

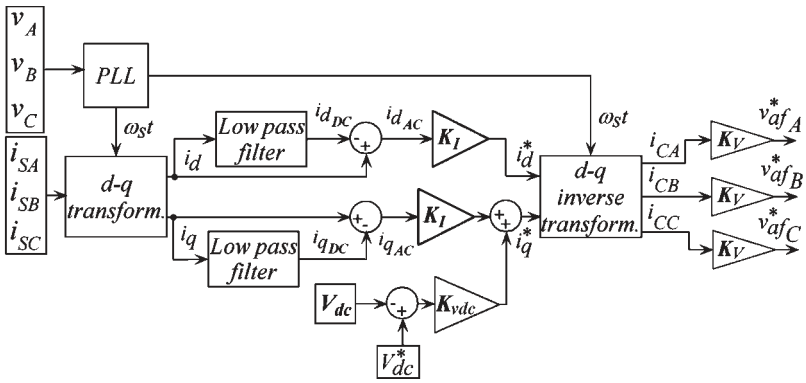

Fig. 7. Control block diagram of the SHAPF.

(i_q) components using a rotating frame synchronous with the positive sequence of the system voltage

$$\begin{bmatrix} i_d \\ i_q \\ i_0 \end{bmatrix} = \frac{2}{3} \begin{bmatrix} \sin(\omega_s t) & \sin\left(\omega_s t - \frac{2\pi}{3}\right) & \sin\left(\omega_s t + \frac{2\pi}{3}\right) \\ \cos(\omega_s t) & \cos\left(\omega_s t - \frac{2\pi}{3}\right) & \cos\left(\omega_s t + \frac{2\pi}{3}\right) \\ \frac{1}{\sqrt{2}} & \frac{1}{\sqrt{2}} & \frac{1}{\sqrt{2}} \end{bmatrix} \begin{bmatrix} i_{\mathrm{SA}} \\ i_{\mathrm{SB}} \\ i_{\mathrm{SC}} \end{bmatrix} \tag{3}$$

where $\omega_s t$ is the phase of the positive sequence of the system voltage and it is provided by a phase-locked loop.

The system under study is a three-wire system where the zero sequence may be neglected, so in the sequel, only i_d and i_q are considered. The active and reactive currents can also be decomposed in their dc and ac values

$$\begin{bmatrix} i_d \\ i_q \end{bmatrix} = \begin{bmatrix} i_{d_{\mathrm{DC}}} \\ i_{q_{\mathrm{DC}}} \end{bmatrix} + \begin{bmatrix} i_{d_{\mathrm{AC}}} \\ i_{q_{\mathrm{AC}}} \end{bmatrix}. \tag{4}$$

The mean values of the instantaneous active and reactive currents $(i_{d_{\mathrm{DC}}}, i_{q_{\mathrm{DC}}})$ are the fundamental active and reactive current components. The ac components of both currents $(i_{d_{\mathrm{AC}}}, i_{q_{\mathrm{AC}}})$ correspond to the contribution of active and reactive harmonic components.

It is desired that the network supplies the dc value of the active current, while its ac component, as well as the reactive current, is supplied by the SHAPF. Considering the reactive current, its dc value is provided by the passive filter, while the VSI provides an ac voltage to damp the harmonics. Then, the instantaneous active and reactive currents are filtered in order to separate both components and generate the correct references to the PWM modulator

$$\begin{bmatrix} i_{d_{\mathrm{AC}}} \\ i_{q_{\mathrm{AC}}} \end{bmatrix} = \begin{bmatrix} i_d \\ i_q \end{bmatrix} - \begin{bmatrix} i_{d_{\mathrm{DC}}} \\ i_{q_{\mathrm{DC}}} \end{bmatrix}. \tag{5}$$

These current components are amplified by a gain K_I.

Aside from providing the harmonic currents, the control system should maintain the dc voltage of the PWM VSI to guarantee its accurate operation. This means to control the active power flow into the power inverter. It is important to notice that no active fundamental current flows through the LC filter. Therefore, the dc voltage control is obtained by controlling the dc value of the reactive current $(i_{q_{\mathrm{DC}}})$ as shown in Fig. 7, where the block diagram of the control system is presented.

Then, the reference currents in the abc frame are

$$\begin{bmatrix} i_{\mathrm{CA}} \\ i_{\mathrm{CB}} \\ i_{\mathrm{CC}} \end{bmatrix} = \begin{bmatrix} \sin(\omega_s t) & \cos(\omega_s t) \\ \sin\left(\omega_s t - \frac{2\pi}{3}\right) & \cos\left(\omega_s t - \frac{2\pi}{3}\right) \\ \sin\left(\omega_s t + \frac{2\pi}{3}\right) & \cos\left(\omega_s t + \frac{2\pi}{3}\right) \end{bmatrix} \begin{bmatrix} i_d^* \\ i_q^* \end{bmatrix}. \tag{6}$$

Each current component is amplified by a gain K_V which corresponds to the voltage gain of the PWM inverter

$$v_{\mathrm{af}}^* = K_V \cdot i_C. \tag{7}$$

The resultant signal v_{af}^* is the voltage reference produced by the control which should be synthesized by the power inverter. Then, the total gain of the SHAPF referred to in the previous section results $K = K_I \ K_V = 60$, where $K_I = 20$ and $K_V = 3$.

D. Passive Filter Connection

The active filter has no control over the reactive compensation. This is fully done by the passive filters. Before connecting the filters, the control starts monitoring the system. When $i_{q_{\mathrm{DC}}}$ is higher than 170 A, the filter tuned at the lowest frequency (seventh in the present case) is attached. If after a transient of three cycles $i_{q_{\mathrm{DC}}}$ continues to be higher than 170 A, the second filter is also connected. Whenever $i_{q_{\mathrm{DC}}}$ falls below 17 A, the second filter is disconnected. If only one filter is actually working and $i_{q_{\mathrm{DC}}}$ is lower that 17 A, the complete filter is removed and no further compensation is performed. It is worth noting that it is not possible to use this filter with light loads below 25% of rated value.

V. Performance Evaluation

In order to evaluate the performance of the proposed filter, the DS under study is simulated for different load conditions.

A. Full Load

First, a maximum demand is considered. This means 20.9 MVA with $\cos\varphi = 0.78$ ($P = 16.3$ MW, $Q = 13$ Mvar). At $t = 0.2$ s, the hybrid filter is connected through the passive filter tuned at the seventh harmonics. The filter tuned at the 11th harmonics is connected after three fundamental cycles, at $t = 0.26$ s. With this configuration, the SHAPF provides a reactive compensation of $Q_C = 6$ Mvar and all the harmonics.

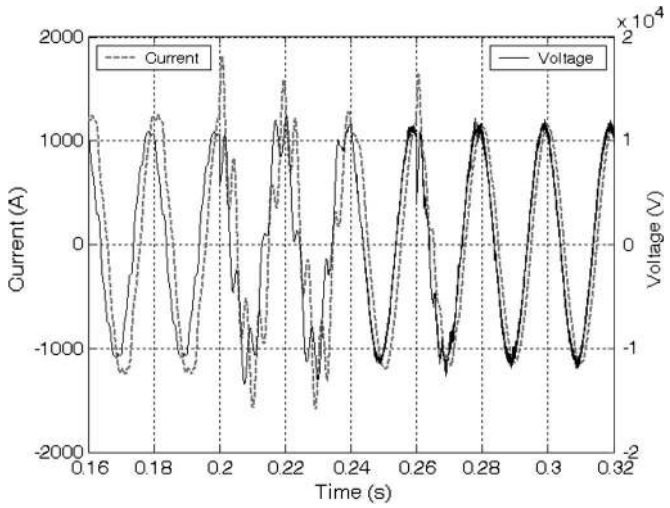

Fig. 8. Full load: Current and voltage at the 13.8-kV bus during the SHAPF connection.

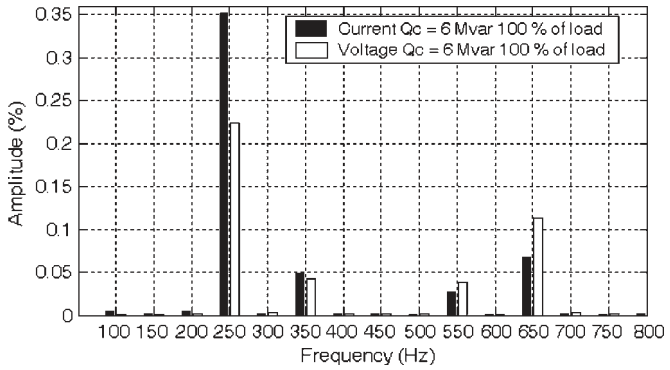

Fig. 9. Full load: Current and voltage spectra at the 13.8-kV bus.

Fig. 8 shows the current and voltage of one phase at the 13.8-kV level upstream of the SHAPF during its connection. A transient behavior, in both current and voltage, is observed after the filter connection, but it lasts less than two fundamental cycles. In addition, a smaller transient appears when the second passive filter is connected. After 80 ms, the benefits of the SHAPF are clearly seen. The supplied current is reduced, while the phase voltage is increased, and it only shows a slight increment of the high-frequency ripple.

Fig. 9 shows the spectra of phase current and voltage at steady state for full-load compensation.

The fundamental current rms value has been decreased to $I_{1\mathrm{rms}} = 804.2$ A, while its THD_I has been reduced to 0.38%. Regarding the voltage harmonics, THD_V has been reduced to 0.56%, while its fundamental rms value is increased to $V_{1\mathrm{rms}} = 8015$ V. Both THDs have been calculated considering up to 12 kHz in order to include the high-frequency harmonics due to PWM switching. When compared with the values given in Table I for $Q_C = 0$ Mvar, there is a decrement of 11% in the fundamental current and an increment of 4% in the fundamental voltage. In addition, both values are slightly better than those obtained with full passive compensation, but with much smaller THDs.

Tables IV and V replicate the results shown in Tables I and II, where the hybrid active filter is used to compensate $Q_C =$ 3 Mvar and $Q_C = 6$ Mvar with 100% of load.

TABLE IV
POWERS AND POWER FACTOR RESULTS

Q_c (Mvar)	P (MW)	Q (Mvar)	V_{1phase} (kV rms)	THD_V (%)	I_{1line} (A rms)	THD_I (%)	$Pf_{tot.}$	Q_{Ac} (Mvar)
3	17	10.5	7868	1.24	847.2	0.76	0.85	3
6	17.7	7.8	8015	0.56	804.2	0.38	0.92	6

TABLE V
RESULTS AND VERIFICATIONS

Harmonic voltages	Q_c 3 Mvar	Q_c 6 Mvar	IEEE limits
V_5 (%)	0.42	0.24	3
V_7 (%)	0.08	0.04	3
V_{11} (%)	0.47	0.04	3
V_{13} (%)	0.65	0.11	3
THD_V (%)	1.24	0.56	5

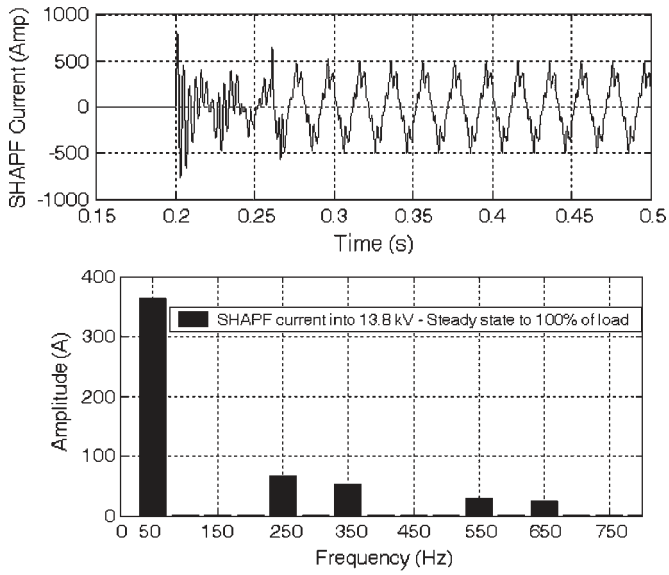

Fig. 10. Full load: PWM VSI current into the PCC and steady-state harmonics.

Both tables clearly show an important improvement in current and voltage total harmonic distortions. When SHAPF is applied, THD_V and the individual harmonics are well below the limits fixed in [21].

Regarding the performance of the PWM VSI, Fig. 10 shows the current delivered by the converter and Fig. 11 shows the dc voltage. Their harmonic components at steady state for full-load compensation are also presented.

The upper trace of Fig. 10 shows the current of one phase entering the PCC, and the bottom trace shows its spectrum. The fundamental component corresponds to the $Q_C = 6$ Mvar reactive compensation, while the harmonics are those required by the load. The switching ripple is almost negligible.

The upper trace of Fig. 11 shows that the dc voltage starts increasing from 0 V immediately after the SHAPF connection. It reaches the reference value of 1.5 kV after 40 ms. The bottom trace shows its spectrum in which the sixth harmonic and its multiples dominate. These correspond to the ac components of the instantaneous active power.

Regarding the power losses of the inverter, the $d-q$ components of the voltage at its output were calculated. For full load, $V_{q_{\mathrm{DCinv}}}$ results equal to 40 V. This means that the inverter losses

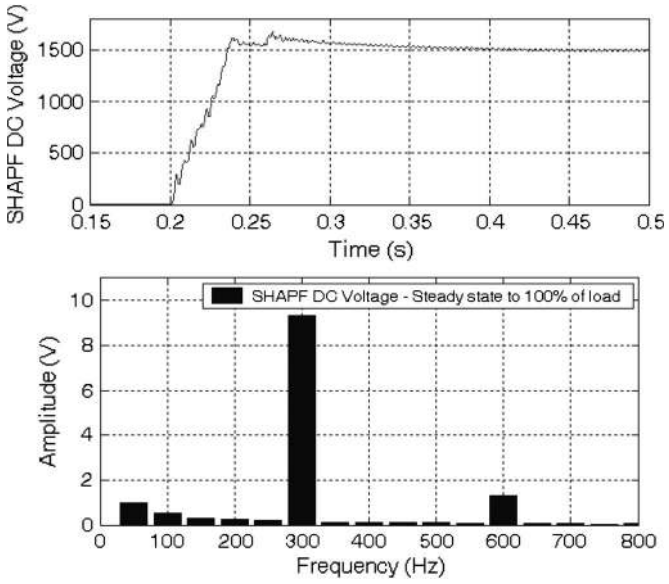

Fig. 11. Full load: DC voltage of the PWM VSI and its steady-state harmonics.

are below 15 kW. That is around 0.2% of the reactive power delivered by the hybrid filter.

B. Load Change

First, a load to the 30% of maximum demand is considered at the 13.8-kV bus. This means 6.27 MVA with $\cos\varphi = 0.78$ ($Pi_{30\%} = 4.89$ MW, $Qi_{30\%} = 3.9$ Mvar). The current harmonic distortion is 30% of its maximum maintaining the relationship with the fundamental value. The hybrid filter is connected through the passive filter tuned at the 7th harmonics, while the filter tuned at the 11th harmonics remains detached. With this configuration, the SHAPF provides a reactive compensation of $Q_C = 3$ Mvar. At $t = 0.45$ s, the load is increased to its maximum demand. This means an increment of 70%, 14.65 MVA with $\cos\varphi = 0.78$ ($Pi_{70\%} = 11.4$ MW, $Qi_{70\%} = 9.17$ Mvar), and a proportional harmonic distortion. Due to the increase of reactive demand, the passive filter tuned at 11th harmonics is connected at $t = 0.46$ s, providing additional $Q_C = 3$ Mvar. With this configuration, the SHAPF provides a reactive compensation of $Q_C = 6$ Mvar and harmonics.

Fig. 12 shows the voltage and current upstream of the SHAPF when the load is increased and the second passive filter is connected. A transient is observed in line voltage and current after the connection of the load and the second passive filter. During the transient, the current increases both its fundamental value and the harmonic distortion. In addition, the phase voltage reduces its amplitude and presents some distortion during this time. In any case, the alterations are not important, particularly considering the severe demand imposed by a 70% of load increment.

The benefits of the SHAPF are clearly seen after a short transient of 40 ms. The supplied current is reduced, while the phase voltage is increased.

Fig. 13 shows the detailed information of phase current and voltage harmonics for a 30% of full load when only one passive filter is connected.

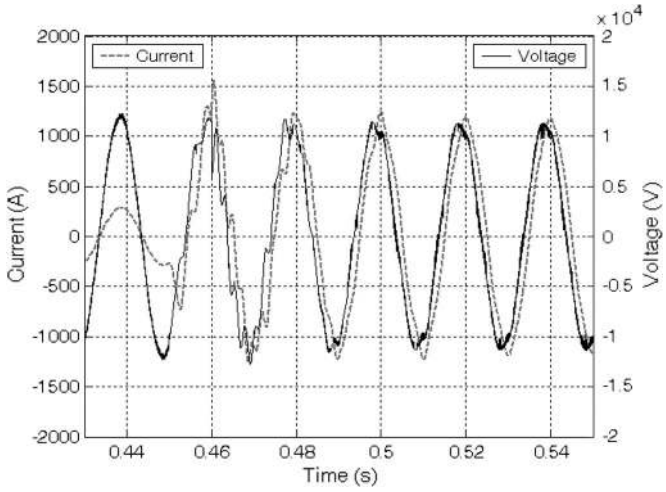

Fig. 12. Load increase: 30% to 100%. Current and voltage in 13.8-kV bus.

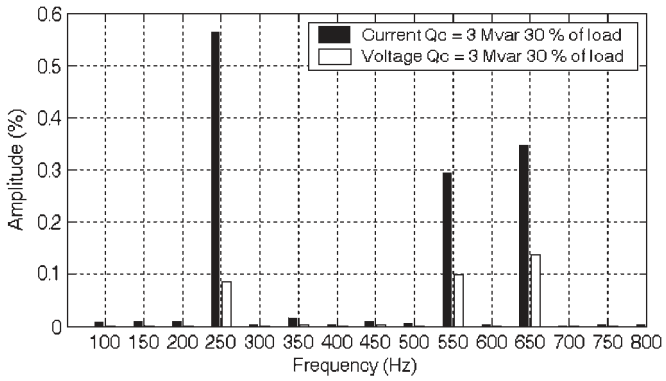

Fig. 13. 30% of full load: Current and voltage spectra at the 13.8-kV bus.

The fundamental rms value of the current has been decreased to $I_{1\mathrm{rms}} = 203.4$ A, while its THD_I has been reduced to 0.74%. Regarding the voltage harmonics, THD_V has been reduced to 0.4%, while its fundamental rms value has been increased to $V_{1\mathrm{rms}} = 8484$ V. Both THDs have been calculated by considering up to 12 kHz in order to include the high-frequency harmonics due to PWM switching.

Regarding the performance of the PWM VSI, Fig. 14 shows the current delivered by the converter and its dc voltage. The upper trace of Fig. 14 shows the current of one phase entering the PCC. A transient of two fundamental cycles is observed when the load is increased and the second passive filter is connected. The fundamental value increases up to the 6-Mvar reactive compensation, while the harmonics are those required by the load. The ripple, due to the switching frequency of the converter, is almost negligible. The bottom trace shows that the dc voltage falls less than 10% when the load is increased, but it quickly recovers the mean value around 1.5 kV. It also presents the sixth harmonic oscillation, due to the ac component of the instantaneous active power.

C. Passive Filter Detuning

The proposed hybrid filter is not very sensitive to the actual tuning of the passive filters. Here, the performance of the proposed filter is evaluated with different detuning of the

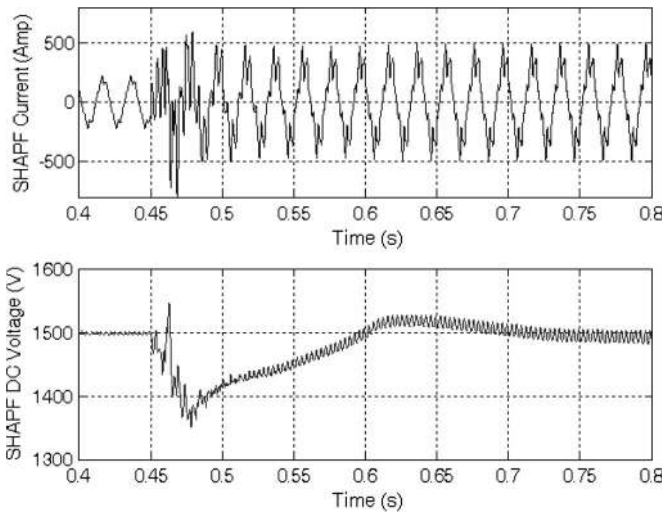

Fig. 14. Load increase: 30% to 100%. PWM VSI current into the PCC and dc voltage.

TABLE VI
CASES OF DETUNING ANALYZED

ΔC_F 7th Passive filter	f_r (Hz)	ΔC_F 11th Passive filter	f_r (Hz)
$C_{F\_7th}(\%) = -15$	$\cong 380$	$C_{F\_11th}(\%) = -15$	$\cong 595$
$C_{F\_7th}(\%) = +15$	$\cong 325$	$C_{F\_11th}(\%) = +15$	$\cong 515$
$C_{F\_7th}(\%) = -15$	$\cong 380$	$C_{F\_11th}(\%) = +15$	$\cong 515$
$C_{F\_7th}(\%) = +15$	$\cong 325$	$C_{F\_11th}(\%) = -15$	$\cong 595$

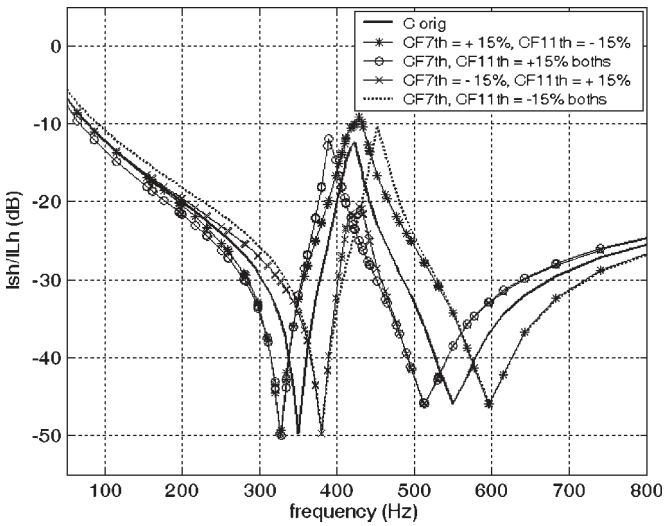

Fig. 15. Filtering characteristics of the hybrid filter with detuning.

passive filters. Table VI shows the different combinations of capacitances that were considered. ΔC_F represents the variation of the filter capacitance with respect to the rated value.

Fig. 15 shows how the filtering characteristics of the hybrid filter are modified when the passive elements are detuned. All the graphics are plotted for $K = 60$. It is clearly seen that even when the resonance frequencies vary a lot, no harmonic amplification occurs.

Figs. 16 and 17 show the spectra of phase current and voltage, at steady state with full-load compensation, for the different cases presented in Table VI together with the original case without detuning.

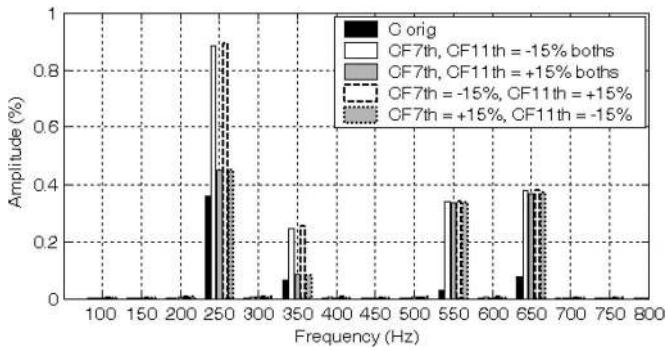

Fig. 16. Full-load detuning: Current spectra at the 13.8-kV bus.

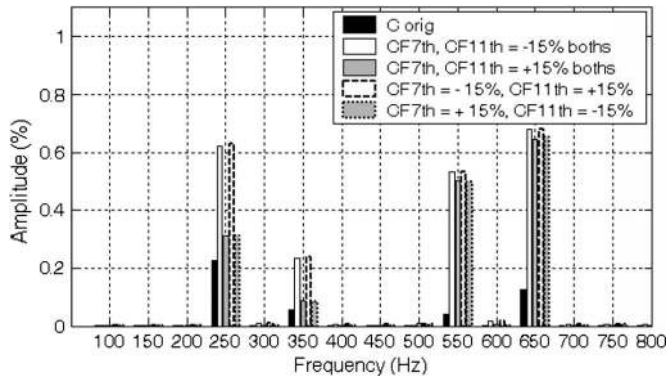

Fig. 17. Full-load detuning: Voltage spectra at the 13.8-kV bus.

The detuning of the lower frequency filter mostly affects the harmonic distortions that remain in the system. THD_v increases up to 1.5% for the lowest capacitance and 1.12% for the highest capacitance. THD_I also raises to 1.01% and 0.67%, respectively. All the results show that the individual harmonics, as well as the THD, remain well below the limits fixed in [21].

VI. CONCLUSION

The design of a shunt hybrid active filter to compensate reactive power and harmonics in the MV level of a power distribution system was presented in this paper. Two levels of reactive compensation were implemented through the design of the passive filter. The first level considered 3 Mvar of reactive compensation supplied by a passive filter tuned at 7th harmonic, while extra 3 Mvar is provided by another passive filter tuned at 11th harmonic. Extra harmonic damping is provided by the active filter in series with them. The proposed filter is rather cheap and simple, and it presents a very good performance in transient and steady-state operation. It represents an excellent solution for the problem presented in the reconfiguration of the distribution network considered in this paper.

REFERENCES

[1] E. Acha, V. G. Agelidis, O. Anaya-Lara, and T. J. E. Miller, *Power Electronic Control in Electrical Systems*, ser. Newnes Power Engineering. Oxford, U.K.: Newnes, 2002.

[2] F. Blaabjerg, R. Teodorescu, M. Liserre, and A. V. Timbus, "Overview of control and grid synchronization for distributed power generation systems," *IEEE Trans. Ind. Electron.*, vol. 53, no. 5, pp. 1398–1409, Oct. 2006.

[3] J. Arrillaga and N. R. Watson, *Power System Harmonics*, 2nd ed. New York: Wiley, 2003.
[4] H. Akagi, E. Watanabe, and M. Aredes, *Instantaneous power theory and applications to power conditioning*, ser. Power Engineering. Piscataway, NJ: IEEE Press, 2007.
[5] B. Singh, K. Al-Haddad, and A. Chandra, "A review of active filters for power quality improvement," *IEEE Trans. Ind. Electron.*, vol. 46, no. 5, pp. 960–971, Oct. 1999.
[6] B. R. Lin and C. H. Huang, "Implementation of a three-phase capacitor-clamped active power filter under unbalanced condition," *IEEE Trans. Ind. Electron.*, vol. 53, no. 5, pp. 1621–1630, Oct. 2006.
[7] L. Moran, J. Mahomar, and J. R. Dixon, "Careful connection, selecting the best point of connection of shunt active power filters in multibus power distribution systems," *IEEE Ind. Appl. Mag.*, vol. 10, no. 2, pp. 43–50, Mar./Apr. 2004.
[8] D. O. Abdeslam, P. Wira, J. Merckle, D. Flieller, and Y. Chapuis, "A unified artificial neural network architecture for active power filters," *IEEE Trans. Ind. Electron.*, vol. 54, no. 1, pp. 61–76, Feb. 2007.
[9] K. K. Shyu, M. Yang, Y. M. Chen, and Y. F. Lin, "Model reference adaptive control design for a shunt active-power-filter systems," *IEEE Trans. Ind. Electron.*, vol. 55, no. 1, pp. 97–106, Jan. 2008.
[10] E. García Canseco, R. Griño, R. Ortega, M. Salichs, and A. Stankovic, "Power factor compensation of electrical circuits," *IEEE Control Syst. Mag.*, vol. 27, no. 2, pp. 46–59, Apr. 2007.
[11] B. Singh, V. Verma, and J. Solanki, "Neural network-based selective compensation of current quality problems in distribution system," *IEEE Trans. Ind. Electron.*, vol. 54, no. 1, pp. 53–60, Feb. 2007.
[12] J. D. Barros and J. F. Silva, "Optimal predictive control of three-phase NPC multilevel converter for power quality applications," *IEEE Trans. Ind. Electron.*, vol. 55, no. 10, pp. 3670–3681, Oct. 2008.
[13] S. Zeliang, G. Yuhua, and L. Jisan, "Steady-state and dynamic study of active power filter with efficient FPGA-based control algorithm," *IEEE Trans. Ind. Electron.*, vol. 55, no. 4, pp. 1527–1536, Apr. 2008.
[14] V. F. Corasaniti, M. B. Barbieri, P. Arnera, and M. I. Valla, "Load characterization in medium voltage of an electric distribution utility related to active filters," in *Proc. IEEE PES TDC*, 2006, pp. 1–7.
[15] V. F. Corasaniti, M. B. Barbieri, P. L. Arnera, and M. I. Valla, "Reactive and harmonics compensation in a medium voltage distribution network with active filters," in *Proc. IEEE ISIE*, 2007, pp. 2510–2515.
[16] R. Inzunza and H. Akagi, "A 6.6-kV transformerless shunt hybrid active filter for installation on a power distribution system," *IEEE Trans. Power Electron.*, vol. 20, no. 4, pp. 893–900, Jul. 2005.
[17] D. Rivas, L. Morán, J. Dixon, and J. R. Espinoza, "Improving passive filter compensation performance with active techniques," *IEEE Trans. Ind. Electron.*, vol. 50, no. 1, pp. 161–170, Feb. 2003.
[18] S. Srianthumrong and H. Akagi, "A medium-voltage transformerless AC/DC power conversion system consisting of a diode rectifier and a shunt hybrid filter," *IEEE Trans. Ind. Appl.*, vol. 39, no. 3, pp. 874–882, May/Jun. 2003.
[19] A. Luo, Z. Shuai, W. Zhu, R. Fan, and C. Tu, "Development of hybrid active power filter based on the adaptive fuzzy dividing frequency-control method," *IEEE Trans. Power Del.*, vol. 24, no. 1, pp. 424–432, Jan. 2009.
[20] IEEE Power Engineering Society Harmonics Working Group, *Tutorial on Harmonics Modeling and Simulation*, 1998. IEEE-PES TP-125-0.
[21] *Recommended Practices and Requirements for Harmonic Control in Electrical Power Systems*, 1993. IEEE Std. 519-1992.
[22] M. Cichowlas, M. Malinowski, M. P. Kazmierkowski, D. L. Sobczuk, P. Rodriguez, and J. Pou, "Active filtering function of three-phase PWM boost rectifier under different line voltage conditions," *IEEE Trans. Ind. Electron.*, vol. 52, no. 2, pp. 410–419, Apr. 2005.
[23] S. R. Bowes and D. Holliday, "Optimal regular-sampled PWM inverter control techniques," *IEEE Trans. Ind. Electron.*, vol. 54, no. 3, pp. 1547–1559, Jun. 2007.
[24] A. Cataliotti, F. Genduso, A. Raciti, and G. Ricco Galluzzo, "Generalized PWM–VSI control algorithm based on a universal duty-cycle expression: Theoretical analysis, simulation results, and experimental validations," *IEEE Trans. Ind. Electron.*, vol. 54, no. 3, pp. 1569–1580, Jun. 2007.
[25] K. M. Cho, W. S. Oh, Y. T. Kim, and H. J. Kim, "A new switching strategy for pulse width modulation (PWM) power converters," *IEEE Trans. Ind. Electron.*, vol. 54, no. 1, pp. 330–337, Feb. 2007.

Victor Fabián Corasaniti (S'05–M'07) received the Electrical Engineer and Master in Engineering degrees from the Universidad Nacional de La Plata (UNLP), La Plata, Argentina, in 1999 and 2008, respectively.

He has been with the IITREE-LAT, Facultad de Ingeniería, UNLP, studying normal and transient conditions of electrical systems and technical planning since 1999. He is currently an Assistant Professor with the Electrical Engineering Department, UNLP. His special field of interest includes power systems operation and control, power quality, and power electronics.

Maria Beatriz Barbieri (M'97–SM'01) received the degree in telecommunications engineering (with honors) from the Universidad Nacional de La Plata (UNLP), La Plata, Argentina, in 1984.

She has been with the IITREE-LAT, Facultad de Ingeniería, UNLP, studying normal and transient conditions of electrical systems and in economic and technical planning since 1983. She is currently a Professor of electricity and magnetism with the Electrical Engineering Department, UNLP. Her special field of interest includes electrical power systems.

Prof. Barbieri is the Argentina PES Chapter Chairman.

Patricia Liliana Arnera (M'99–SM'01) received the degree in electrical engineering from the Universidad Nacional de La Plata (UNLP), La Plata, Argentina, in 1981.

She is currently the Head of IITREE-LAT, Facultad de Ingeniería, UNLP, studying transient conditions of electrical systems and working in electromagnetic fields and health. She is currently a Full Professor of power system with the Electrical Engineering Department, UNLP. Her special field of interest includes electrical power systems.

Prof. Arnera is a member of the Buenos Aires Academy of Engineering in Argentina. She was the Argentina PES Chapter Chairman from 2001 to 2002.

María Inés Valla (S'79–M'80–SM'97) received the Electronics Engineer and Doctor in Engineering degrees from the Universidad Nacional de La Plata (UNLP), La Plata, Argentina, in 1980 and 1994, respectively.

She is currently a Full Professor with the Departamento de Electrotecnia, Facultad de Ingeniería, UNLP, where she is engaged in teaching and research on power converters and ac motor drives. She is also with the Consejo Nacional de Investigaciones Científicas y Técnicas, Buenos Aires, Argentina.

Prof. Valla is a member of the Buenos Aires Academy of Engineering in Argentina. Within the IEEE, she is a Senior Member of the Administrative Committee of the Industrial Electronics Society. She has been a member of the organizing committees of several international conferences.